High-resolution structure of methionine γ-lyase from *Citrobacter freundii*

**Alexei Nikulin,[a] Svetlana
Revtovich,[b] Elena Morozova,[b,c]
Natalia Nevskaya,[a] Stanislav
Nikonov,[a] Maria Garber[b] and
Tatyana Demidkina[b]***

[a]Institute of Protein Research, Russian Academy
of Sciences, 142290 Pushchino, Moscow
Region, Russia, [b]Engelhardt Institute of
Molecular Biology, Russian Academy of
Sciences, Vavilov str. 32, 119991 Moscow,
Russia, and [c]University of Oslo Centre for
Medical Studies, Moscow 117334, Russia

Correspondence e-mail: tvd@eimb.ru

Pyridoxal 5′-phosphate-dependent methionine γ-lyase (MGL) is involved in the metabolism of sulfur-containing amino acids. The enzyme is a promising target in some anaerobic pathogens and is effective in cancer-cell treatment. The structure of the MGL holoenzyme from *Citrobacter freundii* has previously been determined at 1.9 Å resolution. By modification of the crystallization procedure, the previously determined structure of *C. freundii* MGL has been improved to 1.35 Å resolution with R and R_{free} values of 0.152 and 0.177, respectively. This high-resolution structure makes it possible to analyze the interactions between the monomers in detail and to reveal the structurally invariant regions that are responsible for monomer–monomer recognition during the formation of the active enzyme. Details of the mode of cofactor binding and of the flexible regions that may be involved in substrate recognition and binding are also described.

1. Introduction

Methionine γ-lyase (MGL; EC 4.4.1.11) is an enzyme that catalyzes a γ-elimination reaction of L-methionine to produce α-ketobutyric acid, methanethiol and ammonia. In addition to its physiological reaction, the enzyme also catalyzes γ-replacement reactions of L-methionine and its derivatives as well as β-elimination and β-replacement reactions of L-cysteine and S-substituted L-cysteines (Tanaka *et al.*, 1977, 1985).

MGL has been found in a number of bacteria, some of which are anaerobic pathogens (*e.g. Porphyromonas gingivalis, Treponema denticola* and others). It was recently shown that MGL is present in the *Enterobacteriaceae* family, namely in *Citrobacter freundii* (Manukhov *et al.*, 2005). Very recently, it was demonstrated that the enzyme is involved in the catabolism of methionine in *Arabidopsis thaliana* (Rebeille *et al.*, 2006). In the eukaryotic pathogens *Entamoeba histolytica* (Tokoro *et al.*, 2003) and *Trichomonas vaginalis* (McKie *et al.*, 1998), two genes encode MGL enzymes with a sequence identity of around 70% and with differing kinetic properties. Data on the substrate- and reaction-specificity of the enzyme are mainly restricted to the MGLs from *Pseudomonas putida* (Esaki *et al.*, 1977, 1979; Tanaka *et al.*, 1985; Inoue *et al.*, 2000; Takakura *et al.*, 2004), *T. vaginalis* (Lockwood & Coombs, 1991; McKie *et al.*, 1998), *E. histolytica* (Tokoro *et al.*, 2003; Sato *et al.*, 2006) and *C. freundii* (Manukhov *et al.*, 2006; Alferov *et al.*, 2006). The mechanisms of the γ- and β-elimination reactions catalyzed by MGL are not well understood

Table 1
Data-collection and refinement statistics.

Values in parentheses are for the highest resolution shell.

Space group	$I222$
Unit-cell parameters (Å)	$a = 56.45$, $b = 122.80$, $c = 127.92$
Wavelength (Å)	0.843
Resolution (Å)	20–1.35 (1.4–1.35)
Completeness (%)	95.6 (84.5)
$I/\sigma(I)$	20.2 (3.5)
Redundancy	3.8 (3.2)
R_{merge} (%)	3.4 (34.5)
Disordered protein residues	50–54
No. of non-H protein atoms	3169
No. of water molecules	382
No. of unique reflections	95252
R/R_{free}	0.152/0.177
Mean temperature factor B (Å^2)	23.8
R.m.s. deviations from ideal values	
Bond lengths (Å)	0.008
Bond angles (°)	1.02
Chirality angles (°)	0.070
Dihedral angles (°)	16.70
Planarity angles (°)	0.006
Ramachandran plot	
Most favoured (%)	93.7
Additionally allowed (%)	5.7
Generously allowed (%)	0.3
Disallowed (%)	0.3 [Ser190]†

† The conformation of the amino-acid residue at this position is the same in all MGLs and is a characteristic feature of the protein.

compared with those of other PLP-dependent enzymes, particularly aminotransferases (Eliot & Kirsch, 2004).

MGL is of significant interest to medicine as a target in some pathogens and as an antitumour enzyme. It has been demonstrated that trifluoromethionine, an inhibitor of the enzyme, possesses a toxic effect towards pathogens *in vitro* and *in vivo* (Coombs & Mottram, 2001; Yoshimura *et al.*, 2002; Tokoro *et al.*, 2003). The antitumour effect of the enzyme was demonstrated by treatment of cancer cells with the *P. putida* enzyme (Yoshioka *et al.*, 1998) and by gene therapy with the *P. putida* MGL gene in retroviral and adenoviral vectors (Miki, Al-Refaie *et al.*, 2000; Miki, Xu *et al.*, 2000) in combination with MGL. Further mechanistic and structural studies of MGLs from various sources should provide valuable information for both fundamental enzymology and medicine.

MGLs from various sources are composed of four identical subunits with molecular weights of about 43 kDa each. Their primary structures have about 45–60% sequence identity (Manukhov *et al.*, 2006). The crystal structure of MGL was initially solved for the enzyme from *P. putida* (Motoshima *et al.*, 2000). It demonstrated that MGL belongs to the aspartate aminotransferase family of PLP-dependent enzymes with a type I fold (Grishin *et al.*, 1995; Jansonius, 1998) and has features that are characteristic of enzymes of the cystathionine β-lyase subclass (Käck *et al.*, 1999). Recently, the structure of the *P. putida* enzyme at 1.8 Å resolution (Kudou *et al.*, 2007) and preliminary X-ray data for *E. histolytica* MGL (Sato *et al.*, 2006) have been published. The coordinates of *T. vaginalis* MGL and its complex with L-propargylglycine have been deposited in the Protein Data Bank (PDB codes 1e5e and 1e5f). In a previous paper (Mamaeva *et al.*, 2005), the overall crystal structure of MGL from *C. freundii* determined at 1.9 Å resolution was reported. In this paper, we present the crystal structure of MGL from *C. freundii* determined at 1.35 Å resolution. This structure makes it possible to analyze the interactions between the subunits in detail and to reveal the structurally invariant residues that are responsible for dimer and tetramer formation. It also provides us with very precise information about the atom arrangement and distances in the enzyme active centre.
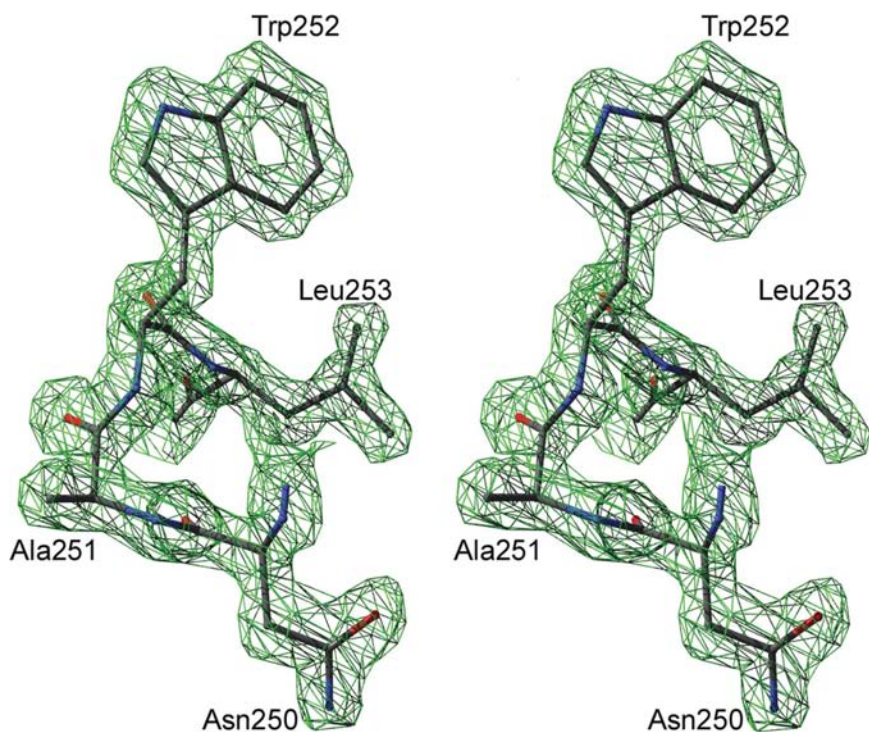
2. Material and methods

2.1. Crystallization and data collection

Methionine γ-lyase from *C. freundii* was isolated and purified as described by Manukhov *et al.* (2005). Crystals of MGL were obtained using the same conditions as described in Mamaeva *et al.* (2005) but without the presence of ammonium sulfate in the solutions. Rhombic shaped crystals appeared after a week and attained dimensions of 0.3–0.4 mm within two weeks. Prior to freezing in liquid nitrogen, the crystals were transferred into cryoprotectant solution (35% MME PEG 2000, 50 m*M* Tris– HCl pH 8.5, 0.2 m*M* PLP, 25 m*M* DTT). Diffraction data were collected at the

Figure 1
Stereoview of a $2F_o - F_c$ electron-density fragment contoured at 3.0σ. The figure was produced using *Swiss-PdbViewer* (Guex & Peitsch, 1997).

EMBL PX beamline BW7B at the DORIS storage ring, DESY (Hamburg, Germany) using a MAR 345 mm image-plate detector and were processed using *XDS* (Kabsch, 1993). The program *BEST* (Bourenkov & Popov, 2006) was used for data-collection optimization. Detailed data-collection statistics are shown in Table 1.

2.2. Structure determination and refinement

The previously determined structure of the protein from *C. freundii* (PDB code 1y4i) was used to solve the MGL structure. Since the space groups of the crystals were identical and the unit-cell parameters were approximately the same, the positions of the protein molecules were also the same as in the previous solved MGL structure. One round of rigid-body refinement was performed in *MOLREP* (Vagin & Teplyakov, 1997). Refinement was carried out with the program *REFMAC* v.5.2.0005 (Murshudov *et al.*, 1997) and rebuilding was performed using the program *Coot* (Emsley & Cowtan, 2004) with σ_A-weighted $2mF_o - DF_c$ and $mF_o - DF_c$ density maps. A free *R* factor calculated from 5% of reflections set aside at the outset was used to monitor the progress of refinement. The flexible loops of the protein and water molecules were removed from the initial model to exclude model bias during the first round of refinement. The *R* and

Figure 2
Crystal structure and sequence of *C. freundii* MGL. (*a*) The tetramer organization of the enzyme. The subunits are shown in green, cyan, grey and orange. PLP covalently bound to Lys210 is shown in red. The tetramer consists of two catalytic dimers (green/cyan and grey/orange). (*b*) Stereoview of a subunit structure. The N-terminal domain is in blue, the central (PLP-binding) domain is in green, the C-terminal domain is in red and PLP is in magenta. Region Phe50–Gly54 is absent from the model. (*c*) Amino-acid sequence of MGL from *C. freundii*. Secondary-structure elements are coloured according to (*b*). Residues that are absent from the model are indicated by dotted lines. Residues that are identical in members of the cystathionine β-lyase subclass are shown with a red background and highly conserved residues are shown with a yellow background; residues that are identical in MGLs from different species are shown with a green background. Residues hydrogen bonded to PLP are indicated by orange triangles. Blue triangles indicate residues that are suggested to organize the substrate-binding pocket. (*a*) and (*b*) and Figs. 3, 4 and 5 were produced using *PyMOL* (DeLano, 2002).
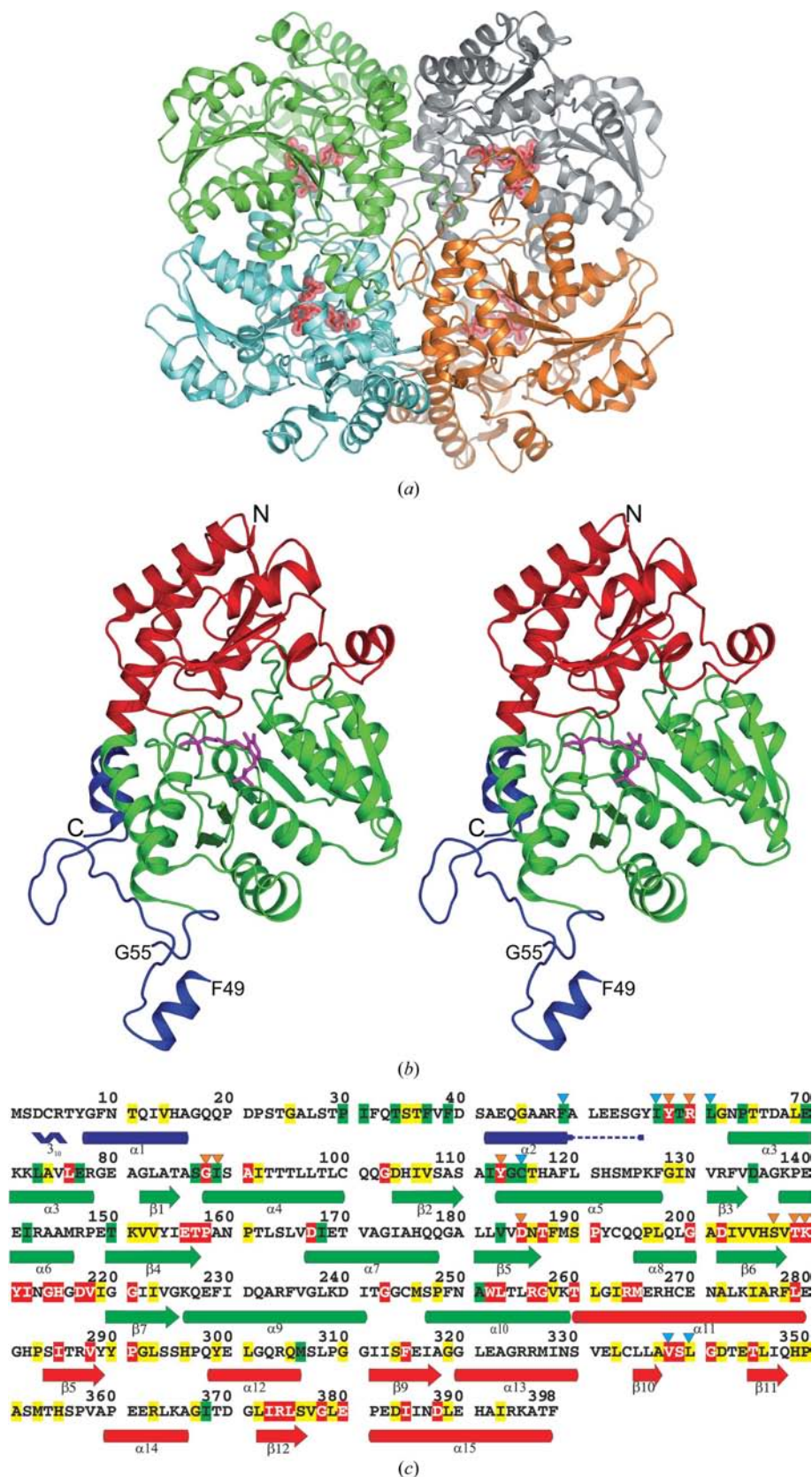
R_{free} factors were 0.24 and 0.26, respectively, at the first round of the refinement.

The electron-density maps were of excellent quality (Fig. 1) and the whole polypeptide chain could be identified apart from several residues of a flexible loop in the N-terminal domain of the protein. An excess of electron density at the S atom of Cys4 forced us to change this residue to *S*-hydroxycysteine. The residue is solvent-accessible and could be easily oxidized. The positions of water molecules were determined using the appropriate procedure implemented in the program *REFMAC*. Alternative positions for 26 amino-acid side chains were incorporated at this stage. The final round of refinement was performed using the *phenix.refine* procedure implemented in the *PHENIX* suite (Adams *et al.*, 2002) with bulk-solvent modelling and individual anisotropic ADP refinement, which improved the *R* and R_{free} factors from 0.194 and 0.209 to 0.151 and 0.177, respectively.

3. Results and discussion

3.1. Overall structure of the methionine γ-lyase

MGL exists as a tetramer in solution (Nakayama *et al.*, 1984) and in crystalline forms (Motoshima *et al.*, 2000; Mamaeva *et al.*, 2005; Fig. 2*a*). The tetramer consists of so-called catalytic dimers related by a twofold axis. The catalytic dimer consists of two subunits related by a twofold axis and includes two active sites. Each active site is formed by amino-acid residues from both subunits and contains PLP. The distance between the two PLP molecules is about 20 Å.

Each monomer consists of three structurally and functionally distinct regions called the N-terminal, PLP-binding and C-terminal domains. The N-terminal domain (residues 1–62) includes a short 3_{10}-helix followed by helices α1 and α2, which are connected by a long loop 17–40 (Figs. 2*b* and 2*c*). The 3_{10}-helix is characteristic of *C. freundii* MGL. The N-terminal domain is connected to the central PLP-binding domain by the long loop 50–62, which participates in the organization of the active site. The large PLP-binding domain (residues 63–259) contains most of the catalytically important residues. The domain has an α/β/α fold with a seven-stranded mainly parallel β-sheet (β1–β7) and eight α-helices (α3–α10) arranged on both sides of the β-sheet. The PLP, which is covalently attached to Lys210, is located near the C-terminal parts of strands β4, β5 and β6. The PLP phosphate group binds near the N-terminus of α4. The PLP-binding domain is connected to the smaller C-terminal domain by the long helix α10. The C-terminal domain (residues 260–398) is comprised of a five-stranded β-sheet (β8–β12) with five α-helices (α11–α15) located on both sides of the β-sheet. Helix α14 is located between the PLP-binding and C-terminal domains and is involved in formation of the PLP-binding site, but this helix makes no direct contacts with the atoms of the PLP-binding domain. The position of helix α14 is similar to that in *P. putida* MGL (Kudou *et al.*, 2007), while in *T. vaginalis* MGL the corresponding helix is located closer to the PLP-binding domain (Messerschmidt *et al.*, 2003).

Table 2
Hydrogen bonds between the subunit molecules of the tetramer.

Molecule 1	Molecule 2	Bond length (Å)	Accessibility	Conservation
Gln33 NE2	Asp217 O	2.96	No	No
Gln33 NE2	Asn250 OD1	3.05	No	No
Thr34 OG1	Gly216 O	3.37	No	Yes
Ser35 N	Gly216 O	2.91	No	Main chain
Thr36 OG1	Ser339 OG	3.11	No	Yes
Thr36 OG1	Asp342 OD2	2.69	No	Yes
Phe39 N	Leu336 O	2.87	No	Main chain
Ala42 N	Asn329 OD1	2.77	No	No
Tyr58 OH	LLP210 O2P	2.53	No	Yes
Arg60 NE	LLP210 O2P	3.01	No	Yes
Thr93 OG1	Ile241 O	2.77	No	No
Leu97 O	Lys126 NZ	2.68	Yes	No
Cys100 O	Lys126 NZ	3.03	Yes	No
Gln102 N	Lys126 O	2.78	No	Main chain

Molecule 1	Molecule 3	Bond length (Å)	Accessibility	Conservation
Gly8 N	Asp384 OD2	2.81	No	No
Phe9 N	Asp381 OD2	3.17	No	No
Asn10 N	Asp381 OD2	2.83	No	No
Thr11 N	Asp381 OD2	3.03	No	No
Thr11 OG1	Asp381 OD2	2.99	No	No
Thr11 OG1	Asp384 OD2	2.58	No	No
Leu253 O	Arg256 NH2	3.14	No	Yes
Arg256 NE	Asp217 OD2	2.66	No	Yes
Arg256 NH2	Asp217 OD1	2.84	No	Yes
Arg256 NH2	Asn213 OD1	2.71	No	No
Arg256 NH2	Leu253 O	3.14	No	Yes
Lys259 NZ	Glu344 OE2	2.84	Yes	No

Molecule 1	Molecule 4	Bond length (Å)	Accessibility	Conservation
Gly25 O	Val38 N	2.78	No	Main chain
Leu27 N	Thr36 O	2.90	No	Main chain
Ile21 N	Ile31 O	2.93	No	Main chain

The catalytic dimer-forming monomers contact each other through large dominantly flat regions. They have a common hydrophobic core and associate tightly through hydrogen bonds (Table 2). The extended region (residues 33–62) of the N-terminal domain, including the long loop and helix α2, stabilizes the catalytic dimer and contains residues that are involved in the formation of the PLP-binding site. Residues Tyr58* and Arg60* of the adjacent monomer make several strong hydrogen bonds to PLP. Residues Gln33*, Thr34* and Thr36* make hydrogen bonds to amino-acid residues of both the PLP-binding and C-terminal domains. Helices α4 and α5 of the PLP-binding domain of both monomers are in close contact with each other; these contacts are mediated by hydrophobic interactions and hydrogen bonds.

The association of the two catalytic dimers results in the formation of the tetrameric structure with four active sites and overall 222 symmetry. This structure is stabilized by an extended network of intermolecular contacts and hydrogen bonds (Table 2). Most of these are provided by the N-terminal domain. Helix α1 makes contacts with the C-terminal domain loops β10/β11 and β12/α15 of the second catalytic dimer. Helix α2 and five preceding residues make contact with β11 and the adjacent loop of the C-terminal domain of another molecule. Residues 28–34 from two catalytic dimers form an

intermolecular two-stranded antiparallel β-sheet structure that stabilizes the whole MGL tetramer. Very important tetramer-forming contacts include four pairs of hydrogen bonds between Asn256 and Asp217 residues that belong to molecules of neighbouring catalytic dimers. These residues are strictly conserved among the PLP-dependent enzymes belonging to the cystathionine β-lyase subclass (Messer-schmidt *et al.*, 2003).

In order to form dimeric and tetrameric structures, an MGL monomer must recognize its partners. Structurally invariant and complementary surface regions are suggested to be used for these purposes. Such regions are formed by strongly conserved residues and their structures are stabilized by intramolecular interactions. Upon complex formation, these residues become inaccessible to the solvent (Nevskaya *et al.*, 2004). We found analogous regions in both the monomer–monomer and dimer–dimer contact areas of the MGL crystal structure. They are constituted by residues of the PLP-binding domain and the C-terminal domain. The first region is formed by residues from helix $\alpha4$ and loops $\beta6/\beta7$ and $\alpha9/\alpha10$; the second contains residues from loops $\beta6/\beta7$, $\beta10/\beta11$, $\beta12/\alpha15$ and helix $\alpha10$. Helix $\alpha1$, loop $\alpha1/\alpha2$ and helix $\alpha2$ of the N-terminal domain, which take part in the formation of both interfaces, predominantly contain nonconserved residues and may possibly be used for additional stabilization of the active enzyme structure.

In *C. freundii* MGL the centre of the tetramer possesses a hydrophobic core involving Phe249, Leu253, Trp252 and Ile31 from all four monomers. The residues of this hydrophobic cluster are not conserved in all subfamily members and can vary to hydrophilic amino acids in some of them. Upon tetrameric structure formation about 30% of the monomer surface becomes inaccessible to solvent.

3.2. PLP-binding site

In each subunit the cofactor-binding pocket is formed by amino acids from its PLP-binding domain (strands $\beta5$ and $\beta6$ and helices $\alpha4$ and $\alpha5$) and from the N-terminal domain of the neighbouring subunit of a catalytic dimer (Fig. 3). The organization of the PLP-binding site is very similar to that found in all known structures of aspartate aminotransferase-family enzymes. Residues Gly88 ($\alpha4$), Tyr113 ($\alpha5$), Asp185 ($\beta5$), Thr209 and Lys210 (loop $\beta6/\beta7$) are identical in all known MGL sequences and residues Tyr58 and Arg60 are strongly conserved (Manukhov *et al.*, 2006).

The main 'anchor' of the cofactor is its phosphate group. In proteins from the aspartate aminotransferase family, PLP is located in the phosphate-binding cap and is surrounded by seven atoms fixing the PLP phosphate handle (Denesyuk *et al.*, 2003). In MGL, four phosphate O atoms are involved in six hydrogen bonds, two of which are bifurcated. Thr209 OG is hydrogen bonded to O1P and the main-chain N atom of Ile89 makes a hydrogen bond to O3P. Ser207 forms a bifurcated hydrogen bond with O1P and O4P, while Gly88 forms a bifurcated hydrogen bond with O1P and O3P (Fig. 3). Two other hydrogen bonds to the PLP phosphate handle are

formed by amino acids of the adjacent subunit of the catalytic dimer. Tyr58* is involved in a hydrogen bond to O2P, while Arg60* NE is hydrogen bonded to the O2P atoms of the phosphate moiety, thus compensating for its negative charge. The position of Arg60* is rather mobile, as in the previously determined structure of *C. freundii* MGL, despite the firmly fixed position of this residue in all other MGL structures, where it makes two strong hydrogen bonds to O2P and O3P. This could be explained by the accessibility of the arginine side chain to water molecules (Table 2).

In the internal aldimine, PLP is covalently attached to Lys210 of the $\beta6$–$\beta7$ loop through the amine N atom. The position of the PLP pyridine ring is stabilized by a hydrogen bond between the N1 atom of the ring and the OD atom of Asp185, which is strictly conserved in the aspartate amino-transferase family. The aspartic acid plays a key role in the stabilization of the positive charge on the pyridine N1 atom, thereby increasing the electrophilic character of the cofactor. The position of the Asp185 side chain is firmly fixed by interaction of the OD atom with the hydroxyl group and the amide N atom of Thr187, thus providing an optimal arrange-ment to interact with the pyridine N atom.

The position of the PLP pyridine ring is supported by Thr187 and Ser207 on one side and by Tyr113 on the other. The side chains of Thr187 and Ser207 lie within a van der Waals distance of the pyridine-ring atoms (about 3.8–3.9 Å), thereby minimizing any cofactor movements in this direction. The phenol ring of Tyr113 is coplanar with the pyridine ring of PLP. Stacking interactions between the two rings, which are 3.5 Å apart, provides additional stabilization of the PLP position. This interaction between an aromatic side chain and the PLP ring system is found in most PLP-dependent enzymes and is believed to increase the electron-sink character of the cofactor (Hayashi *et al.*, 1990; John, 1995; Messerschmidt *et al.*, 2003). The hydroxyl group of Tyr113 makes a single hydrogen bond to the amino group of Arg60*. It was supposed that an analogous interaction in *Escherichia coli* cystathionine β-lyase (Clausen *et al.*, 1996) caused a decrease in the pK_a value of the corresponding tyrosine residue and thus plays an essential role in catalysis by activating the incoming substrate for trans-aldimination in *E. coli* cystathionine β-lyase and in other members of its subclass (Messerschmidt *et al.*, 2003). As in other members of the cystathionine-β-lyase subclass, the C2′-methyl group and the 3′-hydroxyl group of the cofactor are not involved in any interactions with the protein.

PLP is located within a rather deep cavity on the dimer surface (Fig. 4). The entry into the cavity is surrounded by loops $\beta2/\alpha5$ and $\alpha7/\beta5$, helix $\alpha5$ and the C-terminus of helix $\alpha9$ of the central domain and loop $\beta11/\alpha14$ and helix $\alpha14$ of the C-terminal domain. The second subunit of the catalytic dimer is also involved in the formation of this entrance. Its helix $\alpha2$ and the adjacent loop $\alpha2/\alpha3$ of the N-terminal domain protrude towards the entrance and form a flexible flap. The positions of residues 50–54 of loop $\alpha2/\alpha3$ were not determined in the present model. Models of MGL from *P. putida* either do not contain helix $\alpha2$ and the following loop (PDB codes 1gc0 and 1gc2) or the corresponding residues of such models have

B factors that are at least two times higher than the average value for the whole protein because of poor density (PDB codes 1pg8 and 1ukj). In the structures of MGL from *T. vaginalis* (PDB codes 1e5f and 1e5e), the N-terminal loops are well determined but have diverse positions (Fig. 5*a*). Comparison of these MGL structures with those of other members of the enzyme family (Fig. 5*b*) revealed mobility of

this region as well as of the region that includes helix α14 with two adjacent loops and is located at the opposite side of the catalytic pocket. Mobility of these flexible regions surrounding the entrance to the catalytic site could be important for substrate recognition and binding.

Comparison of the active sites of the *C. freundii* MGL structure with the structure of MGL from *T. vaginalis* in a complex with L-propargylglycine (PDB code 1e5e) and the structure of cystathionine β-lyase from *E. coli* in a complex with L-aminoethoxyvinylglycine (PDB code 1cl2; Clausen *et al.*, 1997) reveals the roles of amino-acid residues in binding the substrates. The binding pocket of MGL has a significantly hydrophobic character (Fig. 4*b*), in contrast to that of cystathionine β-lyase (Messerschmidt *et al.*, 2003), owing to the hydrophobic character of the substrate side chain. The binding pocket is organized by residues Tyr113, Cys115, Phe188, Thr209, Val338 and Leu340 from one monomer and residues Phe49*, Ile57*, Tyr58*, Leu61* and Phe235* from the second monomer (Fig. 3). It has been suggested that together with the side chains of Ile57* and Leu61*, the phenyl group of the strictly conserved Phe49* forms a hydrophobic contact area for the methyl group of the methionine substrate (Messerschmidt *et al.*, 2003). Residues Phe235*, Tyr58*, Val338 and Thr209 are present along this hydrophobic line. They
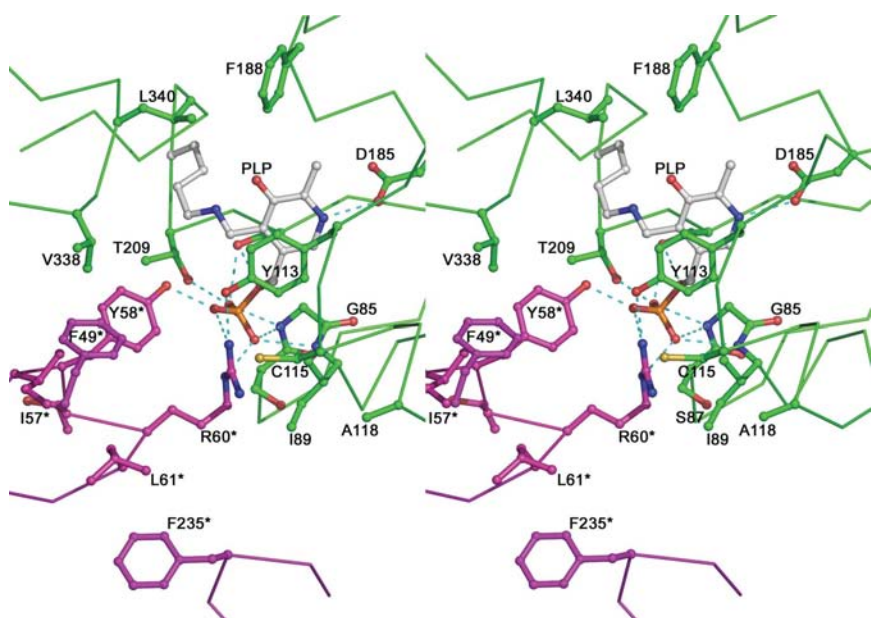

Figure 3
Stereo representation of the MGL active site. Amino-acid residues from the two subunits are shown in green and magenta and the PLP bound to Lys210 is in grey. Residues of the neighbouring subunit are marked with asterisks. Hydrogen bonds are indicated by blue dotted lines.
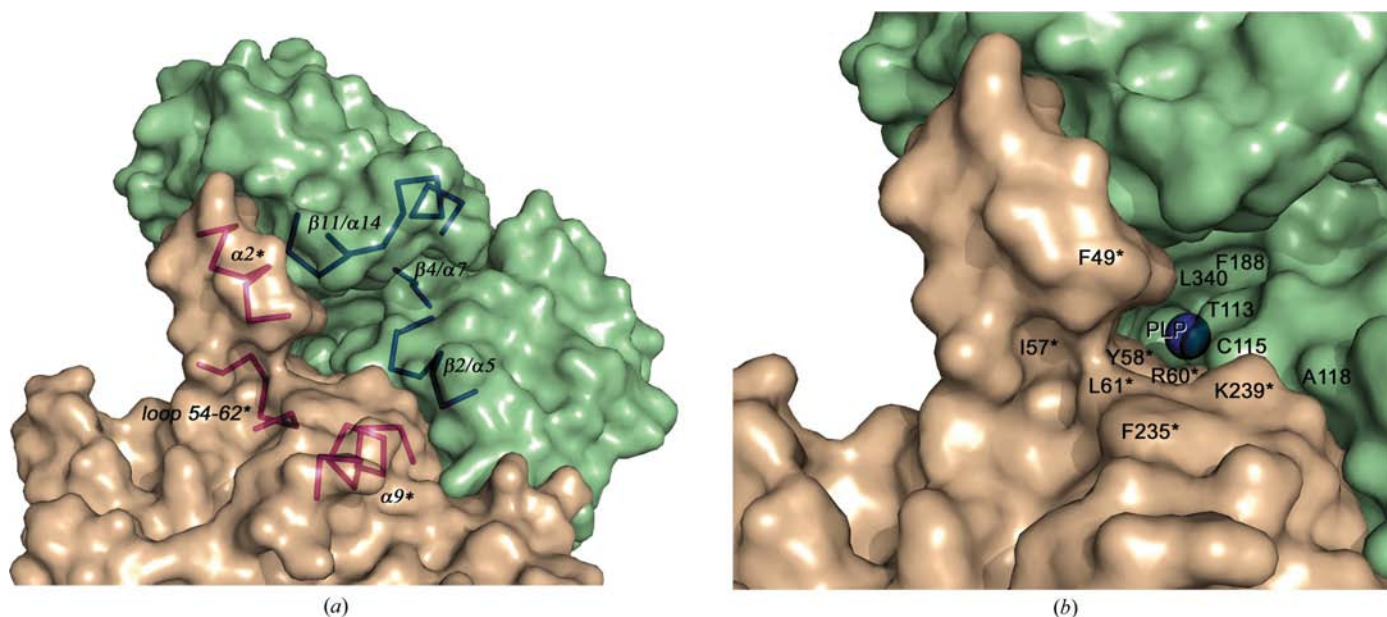

Figure 4
The MGL catalytic dimer interface. (*a*) Solvent-accessible surface. Subunits are shown in green and brown. The secondary-structure elements surrounding the entrance into the PLP-binding pocket are shown in blue and red. (*b*) A close-up view of PLP-binding pocket. Surrounding residues are indicated.
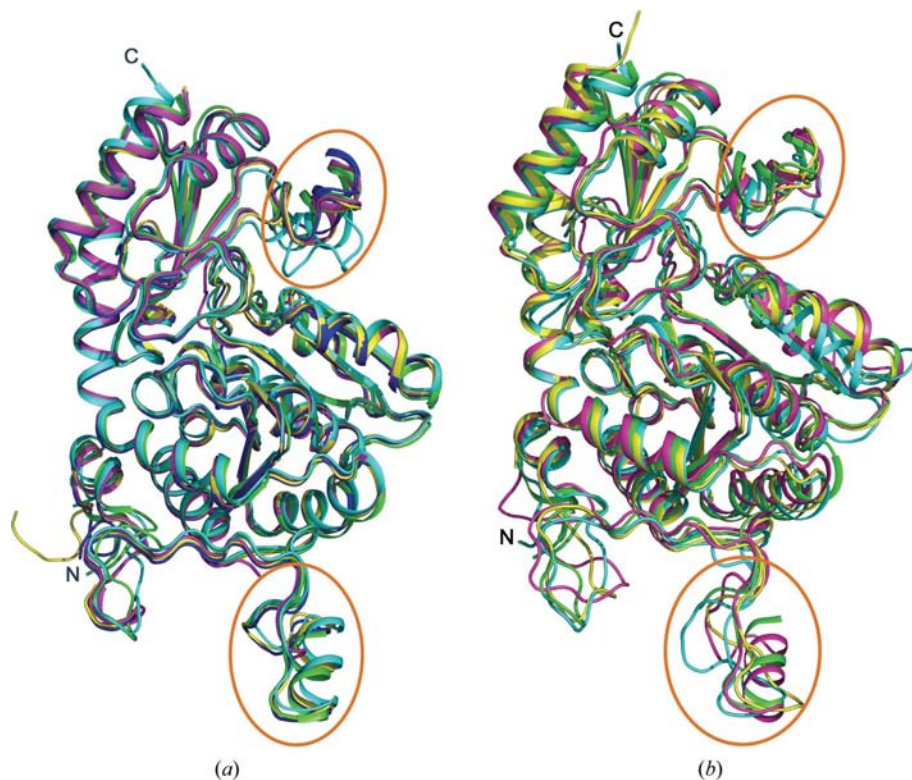
Figure 5
Superposition of the C^{α} traces. (*a*) Crystal structures of MGLs from various species. *C. freundii* MGL (PDB code 2rfv) is in green, *T. vaginalis* MGL (PDB code 1e5f) is in cyan and three *P. putida* MGL structures (PDB codes 1gc0, 1pg8 and 1ukj) are in magenta, yellow and blue. (*b*) Crystal structures of representative cystathionine β-lyase subclass PLP-dependent enzymes. *Saccharomyces cerevisiae* cystathionine γ-lyase (PDB code 1n8p) is in cyan, *Nicotiana tabacum* cystathionine γ-synthase (PDB code 1qgn) is in magenta and *Arabidopsis thaliana* cystathionine β-lyase (PDB code 1ibj) is in yellow. The flexible loops of the N- and C-terminal domains are marked with ovals in both figures.

should be involved in the organization of the hydrophobic patch and the proper positioning of the methionine substrate. Cys115, which is highly conserved in the MGL family (Manukhov *et al.*, 2006), is located opposite these residues. Replacement of the cysteine by glycine reduced the activity of *T. vaginalis* MGL1 and MGL2 towards both methionine and homocysteine by 80–90% (McKie *et al.*, 1998). Substitution of the cysteine by threonine or serine in *P. putida* MGL led to a significant decrease in activity of between 2.5-fold to 11-fold towards both methionine and homocysteine (Kudou *et al.*, 2007). These results demonstrate the importance of the cysteine residue in the γ-elimination reactions catalyzed by MGL. It has been suggested that Cys115 should play an important role in substrate recognition (McKie *et al.*, 1998; Kudou *et al.*, 2007).

As mentioned above, Tyr113 makes a stacking interaction with the pyridine ring of PLP. It has been demonstrated that the tyrosine is important in γ-elimination of the methionine substrate and could play a role as a general acid catalyst in the elimination of the γ-substituent of the substrate (Inoue *et al.*, 2000). Tyr113 could be also involved in the proper positioning of the substrate.

4. Conclusion

We obtained high-quality crystals of *C. freundii* MGL that allowed us to improve the structure of the holoenzyme. The r.m.s. deviation between the 'old' 1.9 Å and the 'new' 1.35 Å models of MGL was 0.80 Å for all C^{α} atoms. Discrepancies are mainly located in the region of the N-terminal loop (residues 55–63), the small flexible loop (residues 159–161) of the PLP domain and the flexible loop (residues 350–368) of the C-terminal domain. The N-terminal loop in the 1.35 Å structure has a gap between residues 49 and 55 because of a lack of electron density. The positions of residues 55–60 differ from the lower resolution model but are close to those of other MGL structures. This results in a change in the positions of the side-chain groups of the PLP-binding residues Tyr58 and Arg60. The main chain of the short loop 159–161 has changed position dramatically. Moreover, several residues of the active site (Tyr113, Glu156, Phe188, Leu340 and Arg374) have diverse conformation in the two structures, whilst PLP retains its position. The high-resolution data allowed the introduction of 382 water molecules instead of the 104 in the 1.9 Å resolution model. Three of the water molecules are located close to PLP, thus modelling the possible position of the substrate at the enzyme active centre.

Comparison of the two structures reveals a very flexible character of the substrate-binding pocket. The high-resolution structure of MGL provides very precise information about the arrangement of atoms and the distances between them in the enzyme active centre. This provides a key to understanding the mechanism of the enzymatic reaction.

References

Adams, P. D., Grosse-Kunstleve, R. W., Hung, L.-W., Ioerger, T. R., McCoy, A. J., Moriarty, N. W., Read, R. J., Sacchettini, J. C., Sauter, N. K. & Terwilliger, T. C. (2002). *Acta Cryst.* D**58**, 1948–1954.

research papers

Alferov, K. V., Faleev, N. G., Demidkina, T. V., Khurs, E. N., Morozova, E. A. & Khomutov, R. M. (2006). *Dokl. Biochem. Biophys.* **407**, 102–105.

Bourenkov, G. P. & Popov, A. N. (2006). *Acta Cryst.* D**62**, 58–64.

Clausen, T., Huber, R., Laber, B., Pohlenz, H. D. & Messerschmidt, A. (1996). *J. Mol. Biol.* **262**, 202–264.

Clausen, T., Huber, R., Messerschmidt, A., Pohlenz, H. D. & Laber, B. (1997). *Biochemistry*, **36**, 12633–12643.

Coombs, G. H. & Mottram, J. C. (2001). *Antimicrob. Agents Chemother.* **45**, 1743–1745.

DeLano, W. L. (2002). *The PyMOL Molecular Graphics System.* DeLano Scientific, Palo Alto, USA. http://www.pymol.org.

Denesyuk, A. I., Denessiouk, K. A., Korpela, T. & Johnson, M. S. (2003). *Biochim. Biophys. Acta*, **1647**, 234–238.

Eliot, A. C. & Kirsch, J. F. (2004). *Annu. Rev. Biochem.* **73**, 398–415.

Emsley, P. & Cowtan, K. (2004). *Acta Cryst.* D**60**, 2126–2132.

Esaki, N., Suzuki, T., Tanaka, H., Soda, K. & Rando, R. R. (1977). *FEBS Lett.* **84** 309–312.

Esaki, N., Tanaka, H., Uemura, S., Suzuki, T. & Soda, K. (1979). *Biochemistry*, **18**, 407–410.

Grishin, N., Phillips, M. A. & Goldsmith, E. J. (1995). *Protein Sci.* **4**, 1291–1304.

Guex, N. & Peitsch, M. C. (1997). *Electrophoresis*, **18**, 2714–2723.

Hayashi, H., Inoue, Y., Kuramitsu, S., Morino, Y. & Kagamiyama, H. (1990). *Biochem. Biophys. Res. Commun.* **167**, 407–412.

Inoue, H., Inagaki, K., Adachi, N., Tamura, T., Esaki, N., Soda, K. & Tanaka, H. (2000). *Biosci. Biotechnol. Biochem.* **64**, 2336–2343.

Jansonius, J. N. (1998). *Curr. Opin. Struct. Biol.* **8**, 759–769.

John, R. A. (1995). *Biochim. Biophys. Acta*, **1248**, 81–96.

Kabsch, W. (1993). *J. Appl. Cryst.* **26**, 795–800.

Käck, H., Sandmark, J., Gibson, K., Schneider, H. & Lindqvist, Y. (1999). *J. Mol. Biol.* **291**, 857–876.

Kudou, D., Misaki, S., Yamashita, M., Tamura, T., Takakura, T., Yoshioka, T., Yagi, S., Hoffman, R. M., Takimoto, A., Esaki, N. & Inagaki, K. (2007). *J. Biochem.* **141**, 535–544.

Lockwood, B. C. & Coombs, G. H. (1991). *Biochem. J.* **279**, 675–682.

McKie, A. E., Edlind, T., Walker, J., Mottram, J. C. & Coombs, G. H. (1998). *J. Biol. Chem.* **273**, 5549–5556.

Mamaeva, D. V., Morozova, E. A., Nikulin, A. D., Revtovich, S. V., Nikonov, S. V., Garber, M. B. & Demidkina, T. V. (2005). *Acta Cryst.* F**61**, 546–549.

Manukhov, I. V., Mamaeva, D. V., Morozova, E. A., Rastorguev, S. M., Faleev, N. G., Demidkina, T. V. & Zavilgelsky, G. B. (2006). *Biochemistry (Mosc.)*, **71**, 361–369.

Manukhov, I. V., Mamaeva, D. V., Rastorguev, S. M., Faleev, N. G., Morozova, E. A., Demidkina, T. V. & Zavilgelsky, G. B. (2005). *J. Bacteriol.* **187**, 3889–3893.

Messerschmidt, A., Worbs, M., Steegborn, C., Wahl, M. C., Huber, R., Laber, B. & Clausen, T. (2003). *Biol. Chem.* **384**, 373–386.

Miki, K., Al-Refaie, W., Xu, M., Jiang, P., Tan, Y., Bouvet, M., Zhao, M., Gupta, A., Chishima, T., Shimada, H., Makuuchi, M., Moossa, A. R. & Hoffman, R. M. (2000). *Cancer Res.* **60**, 2696–2702.

Miki, K., Xu, M., An, Z., Wang, X., Yang, M., Al-Refaie, W., Sun, X., Baranov, E., Tan, Y., Chishima, T., Shimada, H., Moossa, A. R. & Hoffman, R. M. (2000). *Cancer Gene Ther.* **7**, 332–338.

Motoshima, H., Inagaki, K., Kumasaka, T., Furuichi, M., Inoue, H., Tamura, T., Esaki, N., Soda, K., Tanaka, N., Yamamoto, M. & Tanaka, H. (2000). *J. Biochem. (Tokyo)*, **128**, 349–354.

Murshudov, G. N., Vagin, A. A. & Dodson, E. J. (1997). *Acta Cryst.* D**53**, 240–255.

Nakayama, T., Esaki, N., Sugie, K., Beresov, T. T., Tanaka, H. & Soda, K. (1984). *Anal. Biochem.* **138**, 421–424.

Nevskaya, N. A., Nikonov, O. S., Revtovich, S. V., Garber, M. B. & Nikonov, S. V. (2004). *Mol. Biol. (Mosc.)*, **38**, 926–936.

Rebeille, F., Jabrin, S., Bligny, R., Loizeau, K., Gambonnet, B., Van Wilder, V., Douce, R. & Ravanel, S. (2006). *Proc. Natl Acad. Sci. USA*, **103**, 15687–15692.

Sato, D., Yamagata, W., Kamei, K., Nozaki, T. & Harada, S. (2006). *Acta Cryst.* F**62**, 1034–1036.

Takakura, T., Mitsushima, K., Yagi, S., Inagaki, K., Tanaka, H., Esaki, N., Soda, K. & Takimoto, A. (2004). *Anal. Biochem.* **327**, 233–240.

Tanaka, H., Esaki, N. & Soda, K. (1977). *Biochemistry*, **16**, 100–106.

Tanaka, H., Esaki, N. & Soda, K. (1985). *Enzyme Microb. Technol.* **7**, 530–537.

Tokoro, M., Asai, T., Kobayashi, S., Takeuchi, T. & Nozaki, T. (2003). *J. Biol. Chem.* **278**, 42717–42727.

Vagin, A. & Teplyakov, A. (1997). *J. Appl. Cryst.* **30**, 1022–1025.

Yoshimura, M., Nakano, Y. & Koga, T. (2002). *Biochem. Biophys. Res. Commun.* **292**, 964–968.

Yoshioka, T., Wada, T., Uchida, N., Maki, H., Yoshida, H., Ide, N., Kasai, H., Hojo, K., Shono, K., Maekawa, R., Yagi, S., Hoffman, R. M. & Sugita, K. (1998). *Cancer Res.* **58**, 2583–2587.